BIOCHEMISTRY
including biophysical chemistry & molecular biology

Article

pubs.acs.org/biochemistry

Structural Characteristics Determine the Cause of the Low Enzyme Activity of Two Thiopurine *S*-Methyltransferase Allelic Variants: A Biophysical Characterization of TPMT*2 and TPMT*5

Patricia Wennerstrand,[†] Paolo Dametto,[†,∥] Janosch Hennig,[‡,⊥] Therése Klingstedt,[†] Karin Skoglund,[§] Malin Lindqvist Appell,[§] and Lars-Göran Mårtensson*[,†]

[†]Department of Physics, Chemistry, and Biology, Linköping University, SE-581 83 Linköping, Sweden

[‡]Division of Molecular Biotechnology, Department of Physics, Chemistry, and Biology, Linköping University, SE-581 83 Linköping, Sweden

[§]Division of Drug Research/Clinical Pharmacology, Department of Medical and Health Sciences, Faculty of Health Sciences, Linköping University, SE-581 83 Linköping, Sweden

ABSTRACT: The enzyme thiopurine *S*-methyltransferase (TPMT) is involved in the metabolism of thiopurine drugs used to treat acute lymphoblastic leukemia and inflammatory bowel disease. Thus far, at least 29 variants of the TPMT gene have been described, many of which encode proteins that have low enzyme activity and in some cases become more prone to aggregation and degradation. Here, the two naturally occurring variants, TPMT*2 (Ala80 → Pro) and TPMT*5 (Leu49 → Ser), were cloned and expressed in *Escherichia coli*. Far-UV circular dichroism spectroscopy showed that TPMT*2 was substantially destabilized whereas TPMT*5 showed much greater stability comparable to that of wild-type TPMT (TPMTwt). The extrinsic fluorescent molecule anilinonaphthalene sulfonate (ANS) was used to probe the tertiary structure during thermal denaturation. In contrast to TPMTwt, neither of the variants bound ANS to a large extent. To explore the morphology of the TPMT aggregates, we performed luminescent conjugated oligothiophene staining and showed fibril formation for TPMT*2 and TPMT*5. The differences in the flexibility of TPMTwt, TPMT*2, and TPMT*5 were evaluated in a limited proteolysis experiment to pinpoint stable regions. Even though there is only one amino acid difference between the analyzed TPMT variants, a clear disparity in the cleavage patterns was observed. TPMT*2 displays a protected region in the C-terminus, which differs from TPMTwt, whereas the protected regions in TPMT*5 are located mainly in the N-terminus close to the active site. In conclusion, this in vitro study, conducted to probe structural changes during unfolding of TPMT*2 and TPMT*5, demonstrates that the various causes of the low enzyme activity in vivo could be explained on a molecular level.

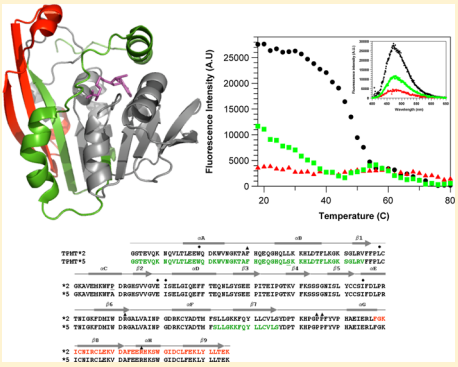

Thiopurines such as azathioprine and 6-mercaptopurine are used to treat acute lymphoblastic leukemia (ALL) and inflammatory bowel disease (IBD). Both of these compounds are prodrugs, and within cells, they are converted to 6-thioguanine nucleotides (6-TGNs) and either are incorporated into DNA or inhibit purine synthesis through the metabolite methyl thioinosine monophosphate.[1,2] The enzyme thiopurine *S*-methyltransferase (TPMT, EC 2.1.1.67) plays an important role in this metabolism, because it metabolically transforms azathioprine and 6-mercaptopurine (6-MP) to methylmercaptopurine and thereby reduces the bioavailability of the 6-TGNs that are incorporated into DNA.

TPMT is a polymorphic enzyme, with at least 29 different allelic variants known today,[3] and it is a classical example of pharmacogenetics in which the TPMT enzyme activities of the allelic variants are directly correlated with the clinical dosages of the thiopurines. Individuals with decreased TPMT activity are at increased risk of developing severe side effects such as bone marrow suppression if they are treated with conventional doses of thiopurines;[4] thus, a 10−15-fold reduction in the size of the dose is required to prevent these adverse events.[5]

The three-dimensional structure of human TPMT has been determined to high resolution (Figure 1A,B).[6] TPMT is a monomeric single-domain protein with a classical Rossman fold.[7] The domain consists of nine β-strands with three helices on each side, and the coproduct *S*-adenosylhomocysteine (SAH) is bound at the carboxyl ends of three parallel β-strands. The mutation sites in the allelic variants are distributed all over the structure, and the structural basis of nonfunctional variants has been discussed[6] and modeled.[8]

Many studies of TPMT have been performed in in vivo systems and have not used purified TPMT variants. On the basis of findings obtained in vivo, it has been suggested, and in a few cases demonstrated,[9,10] that the low enzyme activity

Received: March 23, 2012
Revised: June 28, 2012
Published: June 29, 2012

dx.doi.org/10.1021/bi300377d | *Biochemistry* 2012, 51, 5912−5920

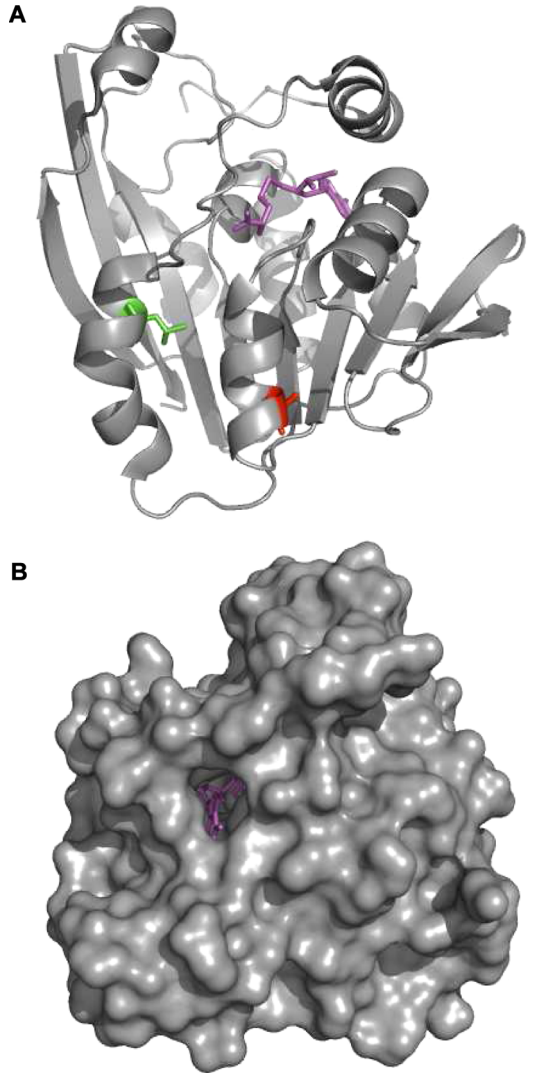

Figure 1. (A) Three-dimensional structure of human TPMT. The positions Ala80 (TPMT*2, red) and L49 (TPMT*5, green) and cofactor SAH (magenta) are indicated. (B) Surface view of TPMT showing the active site cleft (molecule rotated approximately 180° from panel A). This figure was created using the coordinates of PDB entry 2BZG[6] and drawn in PyMOL.[32]

exhibited by most of the allelic variants is the result of the low stability of the protein and/or a stronger tendency to aggregate.

To elucidate if low stability and aggregation are the causes of low enzyme activity, we performed a detailed biophysical characterization.

This study focuses on two naturally occurring variants that have previously been identified: TPMT*2,[11−13] which has a proline substituted for an alanine at position 80, and TPMT*5,[10,13,14] which has a serine substituted for a leucine at position 49. It has been reported that TPMT*2 is rapidly degraded within the cell,[12] whereas TPMT*5 is an outlier variant that shows a strong immunoreactive response (nearly equivalent to that of the wild-type protein) but low enzyme activity.[10]

To characterize the biophysical properties of TPMT*2 (A80P) and TPMT*5 (L49S), these variants were constructed by site-directed mutagenesis and expressed in *Escherichia coli*. Characterization of the variants was achieved by using a variety of biophysical techniques, including far-UV CD spectroscopy, fluorescence spectroscopy, right-angle light scattering, luminescent conjugated oligothiophene staining, and limited proteolysis in conjunction with mass spectrometry.

EXPERIMENTAL PROCEDURES

Construction of TPMT Variants. Human wild-type TPMT and variants thereof were constructed in a truncated version of human TPMT (His6-TPMTΔ14) encoding residues 15−245 and cloned into vector pET-28-Lic, which was generously provided by Structural Genomics Consortium (SGC, Toronto, ON). The variants were constructed using a QuikChange II site-directed mutagenesis kit (Stratagene) according to the manufacturer's instructions. Mutants were verified by DNA sequencing and transformed in *E. coli* strain BL21-Codon plus (DE3)-RIL (Novagen) for large-scale expression.

Large-Scale Expression and Purification. Plasmid pET28-Lic was transformed into *E. coli* BL21-Codon plus (DE3)-RIL competent cells (Stratagene), expressed at 37 °C in LB medium, and induced overnight when the OD_{600} reached 1.0 and the temperature decreased to 21 °C. Thereafter, the cells were lysed by sonication and purified at 4 °C using Ni-NTA Superflow (Qiagen). To remove the His tag, the protein was cleaved by biotinylated thrombin (Novagen) and separated on a Superdex 200 10/30 column (GE Healthcare Biosciences). The protein was stored at −80 °C in 20 mM potassium phosphate buffer (pH 7.3), 150 mM NaCl, 0.5 mM tris(2-carboxyethyl)phosphine (TCEP), and 10% glycerol.

Enzyme Activity Measurements. The enzyme activity of all the TPMT variants was measured according to the recently described protocol.[15]

Circular Dichroism Measurements. All CD spectra were recorded on a Chirascan (Applied Photophysics). In the far-UV region, the protein [3 μM in 20 mM potassium phosphate (pH 7.3), 75 mM NaCl, 2% glycerol, and 0.5 mM TCEP] was placed in a thermostated 0.4 cm path-length cuvette, and far-UV CD measurements (spectrum from 200 to 260 nm) were performed. To assess the stability in the far-UV region, the ellipticities at 222 nm were monitored every 2 °C from 18 to 80 °C, with an equilibration time of 1 min between each measurement and 10 scans at each temperature.

Fluorescence Measurements. To probe the anilinonaphthalene sulfonate (ANS) binding while increasing the temperature, ANS (20-fold molar excess over the protein) was added to the protein samples [3 μM in 20 mM potassium phosphate (pH 7.3), 75 mM NaCl, 2% glycerol, and 0.5 mM TCEP], and then the samples were incubated for 10 min at room temperature. The excitation wavelength was 360 nm, and emission spectra were recorded at 400−600 nm. Thermal denaturation was assessed by monitoring the fluorescence intensity at 475 nm at various temperatures.

Right-Angle Light Scattering. Right-angle light scattering during the temperature increase was measured for all three TPMT variants [3 μM protein in 20 mM potassium phosphate (pH 7.3), 75 mM NaCl, 2% glycerol, and 0.5 mM TCEP]. This was done using an excitation wavelength of 330 nm and an emission wavelength of 332 nm, with a 1 nm slit and an equilibration time of 1 min between each temperature.

Luminescent Conjugated Oligothiophene (LCO) Staining. A 50 μL aliquot of the aggregated sample from right-angle light scattering was stained with 0.5 μM heptaformic thiophene acetic acid (h-FTAA) for 24 h at 4 °C. Thereafter, 2 μL of the sample was placed on a microscope slide and allowed

dx.doi.org/10.1021/bi300377d | *Biochemistry* 2012, 51, 5912−5920

to dry before being mounted with mounting medium and visualized in a Leica DM6000 B fluorescence microscope (Leica) equipped with a SpectraCube module (Applied Spectral Imaging). Emission spectra were recorded from 500 to 700 nm using an excitation wavelength of 480 nm. Emission peaks at 542 and 587 nm were used to quantify protein aggregation.

Limited Proteolysis Experiment. The limited proteolysis experiments were conducted as described previously.[16,17] In short, all TPMT variants were subjected to proteolytic digestion by chymotrypsin at 37 °C. The cleavage was conducted in the same buffer that was used in other measurements. The concentration of the TPMT variants was 15.6 μM, and the optimal protein:protease ratio (determined in range finding experiments) was 8:1. Reactions were stopped by adding a 0.1% trifluoroacetic acid/50% acetonitrile mixture after 0, 1, 2, 5, 10, 20, 50, 100, and 200 min. All experiments were performed in duplicate. A sample from each time point was mixed with the α-cyanocinnamic acid matrix at a 1:1 ratio directly on the sample plate and then analyzed on an Applied Biosystems Voyager mass spectrometer. Fragments were analyzed by using MTMDAT[18] to construct three-dimensional plots from the relative peak intensities, based on a published algorithm.[16]

Theoretical Structural Analysis. The potential structural effects of the TPMT*2 and TPMT*5 variants were investigated using SIFT (available at http://sift.jcvi.org/). This algorithm predicts whether an amino acid substitution will influence protein function based on sequence homology and the physical properties of amino acids. Probability scores of <0.05 suggest deleterious amino acid changes.[19] Proteins homologous to TPMT were identified by performing a SIFT search in the protein databases SWISSPROT 51.3 and TREMBL 34.3. The SIFT software recommends that a median sequence conservation of 2.75−3.25 be used to avoid false-positive results. For TPMT, a median sequence conservation of 3.01 was found by aligning 21 homologous proteins.

RESULTS

Analysis of Structural Changes Using Circular Dichroism. Far-UV circular dichroism (CD) spectroscopy (Figure 2) was performed on wild-type TPMT (TPMTwt), TPMT*2, and TPMT*5 at 18 °C to monitor the possible structural differences caused by the amino acid substitutions. At this temperature, both variants were enzymatically active, albeit less active than TPMTwt with enzyme activities of 47% (TPMT*2) and 14% (TPMT*5) compared to that of TPMTwt (corresponding values at 37 °C were 37 and 0.3%, respectively). TPMTwt displayed a minimum at a wavelength of 222 nm (Figure 2), which reflects the α-helical content of the protein and is similar to results reported by other investigators.[9] Compared to TPMTwt, TPMT*2 had a markedly different CD spectrum that displayed a broader minimum shifted to lower wavelengths and a higher amplitude (Figure 2). On the other hand, the spectrum of TPMT*5 was similar to that of TPMTwt but with a lower amplitude (Figure 2).

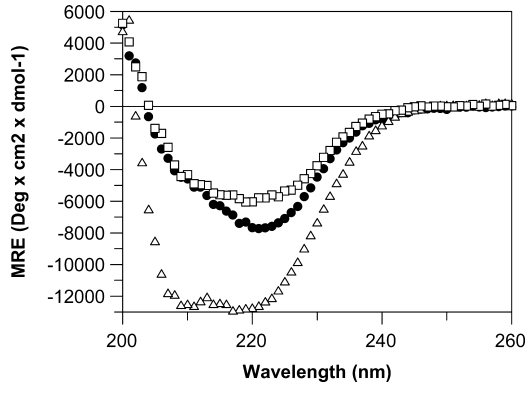

Figure 2. Far-UV CD spectra of TPMTwt (●), TPMT*2 (△), and TPMT*5 (□).

The mutation sites in TPMT*2 and TPMT*5 are situated in α-helices (Figure 1A). The observed differences in the far-UV CD spectra of these variants suggest changes in the secondary structure of these proteins. It is also possible that the disparities between the far-UV CD spectra are the result of changes in the environment of tryptophan residues in these variants. It has previously been demonstrated that aromatic residues, especially Trp residues, contribute significantly to the far-UV CD spectra,[20] and one or two Trp residues (Trp78 and Trp150) are located close to the mutation sites in TPMT*2 and TPMT*5, respectively.

To monitor the stability and changes in secondary structure content, we conducted temperature-induced denaturation at a wavelength of 222 nm (Figure 3). The results showed that

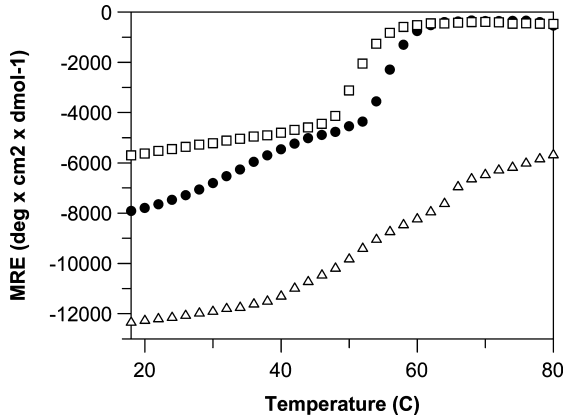

Figure 3. Thermal denaturation using far-UV CD spectroscopy monitored at 222 nm of TPMTwt (●), TPMT*2 (△), and TPMT*5 (□).

TPMTwt unfolds in two steps, with the first transition at an approximately physiological temperature where the enzyme is fully active, followed by a distinct thermal transition midpoint of denaturation (T_m) at ~55 °C. In contrast, TPMT*5 showed only one distinct transition at a T_m of ~50 °C, and TPMT*2 displayed a gradual decrease in the magnitude of its CD signal and no pronounced cooperative transition. At the end of the run, aggregates were clearly visible in the cuvette for all variants but were more pronounced for TPMT*2. This disparity in aggregation behavior exhibited by TPMT*2 is reflected by the light scattering at 80 °C in the CD spectrum.

Analysis of Structural Changes by Binding of Anilinonaphthalene Sulfonate (ANS). Although the natural substrate is not known, TPMT can catalyze methyl-transfer reactions for a variety of substrates involved in thiopurine metabolism. To explore the flexibility of the binding site cavity of 6-mercaptopurine (6-MP) and *S*-adenosylmethionine (SAM), ANS was used as an extrinsic fluorescent hydrophobic probe. ANS is the classical extrinsic fluorescent probe for

dx.doi.org/10.1021/bi300377d | *Biochemistry* 2012, 51, 5912−5920

monitoring the hydrophobic patches during denaturation.[21,22] In contrast to many other globular proteins, TPMT and other members of the methyltransferase family (e.g., adenine methyltransferase) strongly bind ANS under native conditions.[23]

The active site region of TPMT consists of a large hydrophobic cavity that can be easily accessed from the surface of the protein,[6] and it has been demonstrated that the cofactor SAM can be replaced by ANS in other members of the methyltransferase family.[23,24] These observations show that the binding surfaces of SAM and ANS are similar.

A thermal denaturation study of the TPMT variants was conducted by adding ANS and monitoring the decrease in fluorescence intensity caused by the heat-induced loss of ANS binding (Figure 4). In the native state, TPMTwt bound ANS

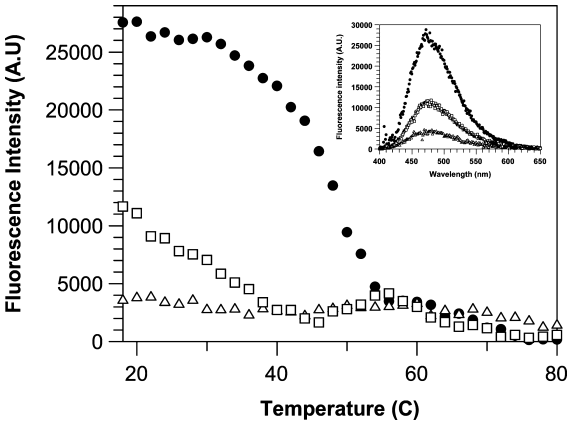

Figure 4. Thermal denaturation using fluorescence spectroscopy with ANS as an extrinsic probe for TPMTwt (●), TPMT*2 (△), and TPMT*5 (□). The inset shows the emission spectra of the TPMT variants under native conditions monitored at 400−650 nm.

most strongly whereas TPMT*2 and TPMT*5 showed 86 and 58% decreases in fluorescence intensity, respectively, compared to that of TPMTwt (Figure 4, inset). Thermal denaturation of TPMTwt in the presence of ANS displays a two-state transition with a T_m value of ∼50 °C. Neither TPMT*2 nor TPMT*5 exhibited a pronounced cooperative transition (Figure 4), which shows that the binding sites are already affected in the native state.

Right-Angle Light Scattering. The low enzyme activity of TPMT*2 and TPMT*5 might be explained by the ability of these proteins to form aggregates, a behavior that has previously been reported for other TPMT variants.[9,15] To address that issue, a right-angle light scattering experiment was performed to monitor the formation of aggregates as a function of an increasing temperature (Figure 5). In general, all three variants used in this study are prone to aggregation under conditions with increasing temperatures, and the onset of aggregation occurs at 42−52 °C, which is in contrast to the behavior of our recently published variant TPMT*28 (rs 79901429).[15] In these experiments, TPMTwt and TPMT*5 showed onsets of aggregation at 52 and 48 °C, respectively, and similar amplitudes of the fluorescence signal and end value. By comparison, TPMT*2 exhibited an onset of aggregation at 42 °C and a different aggregation profile upon exposure to increased temperatures. Notably, for all three TPMT variants, the onset of aggregation accompanied the denaturation profile observed by far-UV CD spectroscopy.

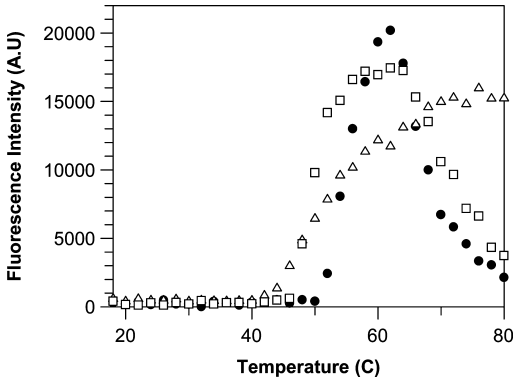

Figure 5. Right-angle light scattering at increased temperatures for TPMTwt (●), TPMT*2 (△), and TPMT*5 (□).

Luminescent Conjugated Oligothiophene (LCO) Staining. To further study the differences in the aggregation behavior of the variants, we performed fluorescence microscopy using luminescent conjugated oligothiophenes (LCOs) as fluorescent molecules in an attempt to probe the structures of the aggregates.[25,26] In this analysis, thermally denatured samples from the right-angle light scattering measurements were incubated with LCO h-FTAA. In the fluorescence images (Figure 6), the aggregate morphology observed upon binding of h-FTAA differed between the TPMT variants. TPMTwt showed weak binding of h-FTAA (fast photobleaching), monitored as an emission spectrum with a low fluorescence intensity and less well-resolved spectral peaks, whereas TPMT*5 displayed stronger binding of h-FTAA, indicated by more pronounced spectra and different shapes of the aggregates (Figure 6). Compared to TPMTwt, TPMT*2 exhibited a markedly different morphology and displayed a high fluorescence intensity caused by stronger binding of h-FTAA and two distinct peaks in the emission spectra characteristic of aggregated protein.[25,26]

Probing Flexibility by Limited Proteolysis. Chymotrypsin was used in a limited proteolysis approach to probe the flexibility or local unfolding of the TPMT variants. Chymotrypsin has a preference for cleavage at aromatic and bulky hydrophobic residues, and there are 53 such potential cleavage sites in TPMTwt. In this experiment, TPMTwt, TPMT*2, and TPMT*5 were incubated under identical conditions for different lengths of time (0−200 min), and the resulting peptide masses were measured by MALDI-TOF mass spectrometry and assigned to their corresponding sequence using MTMDAT.[18] The altered amino acids in both TPMT*2 and TPMT*5 are situated in helices, and even though these two variants differ by only one amino acid, clear dissimilarities was observed between their relative cleavage patterns (Figure 7). To analyze the flexibility and rigidity of the variants, the differences in cleavage patterns after proteolytic digestion of the proteins were evaluated. The picture that emerged from the cleavage analysis pinpointed differences in structure among the three variants.

The regions with an increased relative propensity for cleavage at the end of the incubation were interpreted as being stable. TPMT*2 displayed such a stable region between residues 208 and 245 in the C-terminus, and this was not observed in TPMTwt. TPMT*5 had two stable regions, one consisting of residues 15−65 and the other of residues 173−186, which were

dx.doi.org/10.1021/bi300377d | Biochemistry 2012, 51, 5912−5920

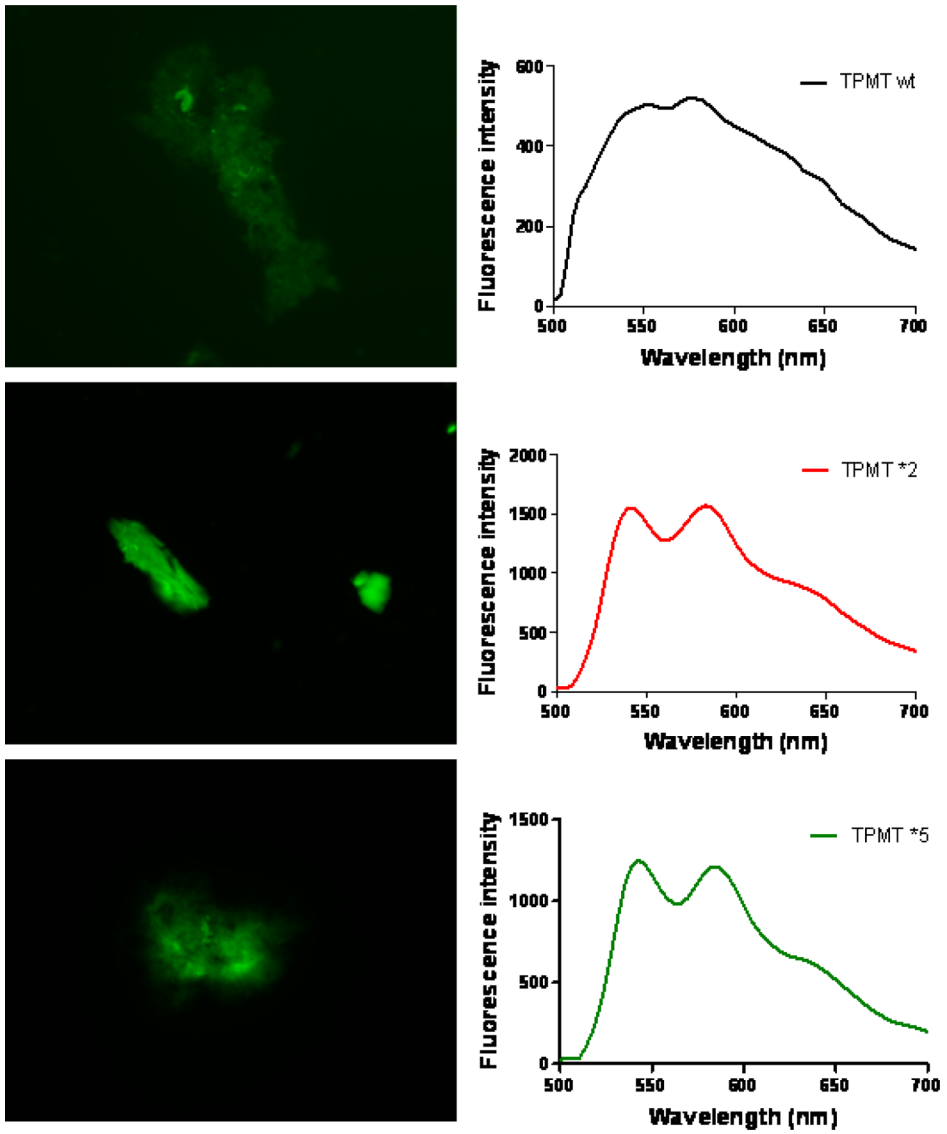

Figure 6. Fluorescence images of protein aggregation of the TPMT variants stained with LCO h-FTAA and their corresponding emission spectra. Because of differences in the fluorescence intensities of the samples, the exposure times varied and were 78, 46, and 60 ms for TPMTwt, TPMT*2, and TPMT*5, respectively.

also noticeable in the other two variants, albeit to a lesser extent (Figures 7 and 8A,B).

■ DISCUSSION

Human TPMT has been studied fairly extensively, and several new allelic variants are detected and published every year (http://www.imh.liu.se/tpmtalleles).

In common for most of the detected variants are low enzyme activities. Two variants, TPMT*2 and TPMT*5, were used in this study, and both exhibit low enzyme activity in vivo. However, in vitro cell studies have shown that TPMT*2 is degraded rapidly[12] whereas TPMT*5 displays a strong immunoreactive response,[10] almost as strong as that of TPMTwt, indicating a similar native fold.

In this work, we provide data to distinguish the biophysical properties of TPMT*2 and TPMT*5 to understand the structural characteristics causing low enzyme activity in vivo.

Even though TPMT is a well-studied protein, there are only a few reports dealing with biophysical characterization of TPMT.[9,13,15,27,31] To the best of our knowledge, this study represents the most comprehensive biophysical characterization of two TPMT variant alleles.

The proline at position 80 (TPMT*2) and the serine at position 49 (TPMT*5) are located in two neighboring helices 16.2 Å (TPMT*2) and 11.3 Å (TPMT*5), respectively, from the coproduct SAH (measured from the Cα atom of the TPMTwt).[6] Both helices are highly conserved (Figure 9), and modeling with the sorting intolerant from tolerant (SIFT) algorithm[19] demonstrated theoretical SIFT scores of 0.00 and 0.03 for positions Leu49 and Pro80, respectively, which predict effects on protein function.

The estimated yield of TPMT*5 after purification was ~35 mg of pure protein/L of culture medium, a level similar to or slightly lower than the yield of TPMTwt. Under identical purification conditions, the yield of TPMT*2 was significantly lower, ~1.5 mg of pure protein/L of culture medium, which reflects the low intrinsic stability of this variant.[12]

Far-UV CD spectra (Figure 2) show native secondary structure similarities between TPMTwt and TPMT*5, whereas a clear difference was observed for TPMT*2, which had a

dx.doi.org/10.1021/bi300377d | Biochemistry 2012, 51, 5912−5920

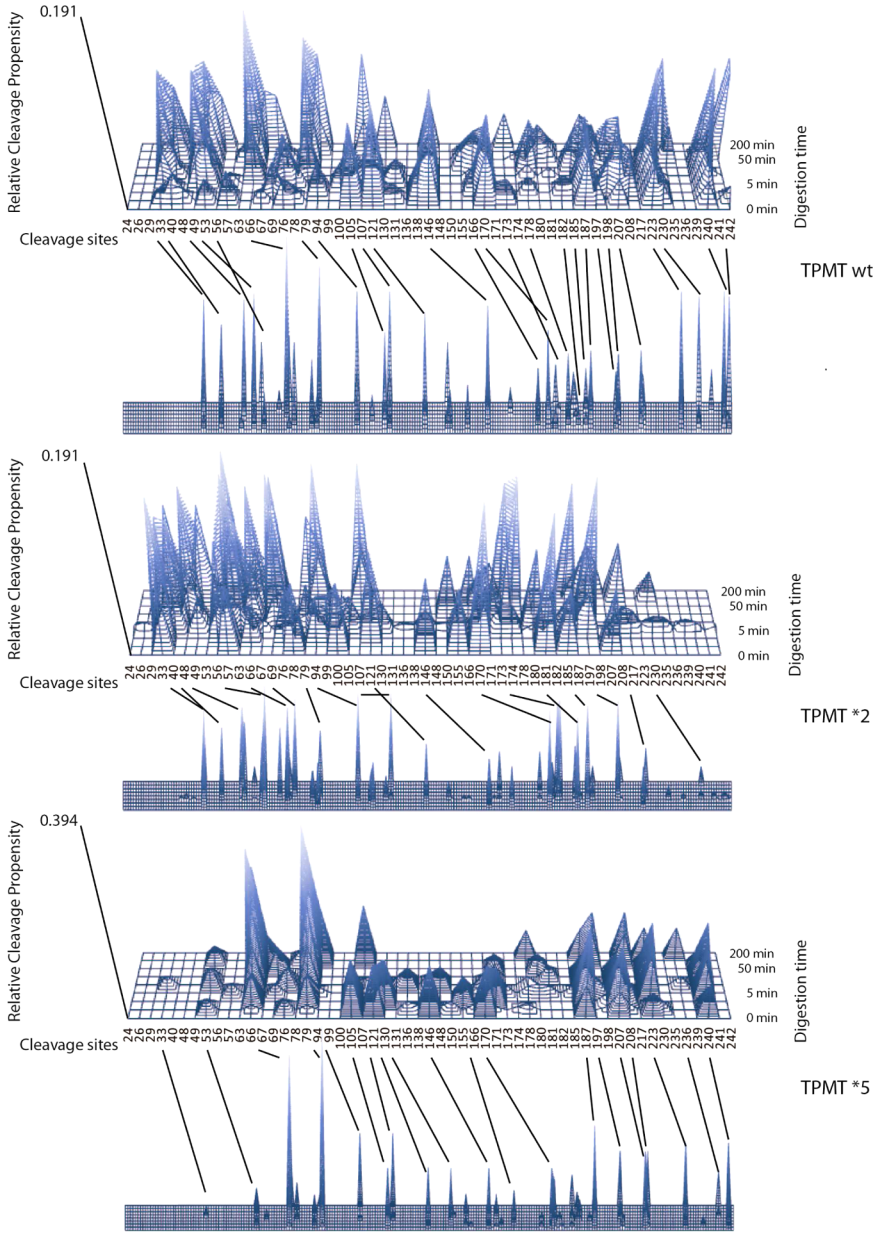

Figure 7. Three-dimensional representation of relative cleavage propensities of wild-type TPMT and its variants as assessed by mass spectrometry. Relative cleavage propensities of the wild-type protein are shown in the top panel, those of TPMT*2 in the middle panel, and those of TPMT*5 in the bottom panel. Each panel is divided into two graphs; the larger top graph shows only propensities for cleavage sites being cut in any of the three variants, whereas the bottom graph includes all residues in the amino acid sequence. The black lines between the graphs connect the corresponding residues. To allow comparison of the panels, the scale of the axis of relative cleavage propensities shows the value of the highest propensity.

higher amplitude probably reflecting oligomerization. Far-UV CD thermal denaturation was conducted to probe disruption of the secondary structure. The observed transition for TPMTwt was interpreted as being a nonideal two-state transition, with a "pre-transition" due to secondary structure rearrangement at physiological temperature where the TPMTwt is fully active. The observed pre-transition has been noted earlier but not analyzed.[6,9] The low stability of TPMT*2, with no clear transition midpoint, explains the low enzyme activity at physiological temperature where the lack of a distinct transition for TPMT*2 resembles what has previously been described for TPMT*3A aggregates.[9] TPMT*5, on the other hand, displayed a two-state transition with a thermal midpoint similar to that of TPMTwt; hence, the low enzyme activity cannot be explained by changes in the secondary structure or stability.

The different ANS binding properties of the TPMT variants (Figure 4, inset) in the native state and immediately after the initiation of thermal denaturation illustrate that TPMT*2 and TPMT*5 clearly differ from TMPTwt with regard to flexibility and changes in tertiary structure. TPMTwt displayed a distinct transition at a T_m value of ~50 °C, similar to the T_m value determined by far-UV CD analysis that demonstrates that the loss of ANS binding accompanied the loss of secondary structure.

The low capacity of ANS to bind TPMT*2 is probably reflected by the low intrinsic stability of this variant. Interestingly, the T_m obtained from the far-UV CD thermal denaturation and those obtained by analyzing ANS binding during thermal melts differed markedly for TPMT*5. Obviously, substitution of a leucine at position 49 has caused

dx.doi.org/10.1021/bi300377d | *Biochemistry* 2012, 51, 5912−5920

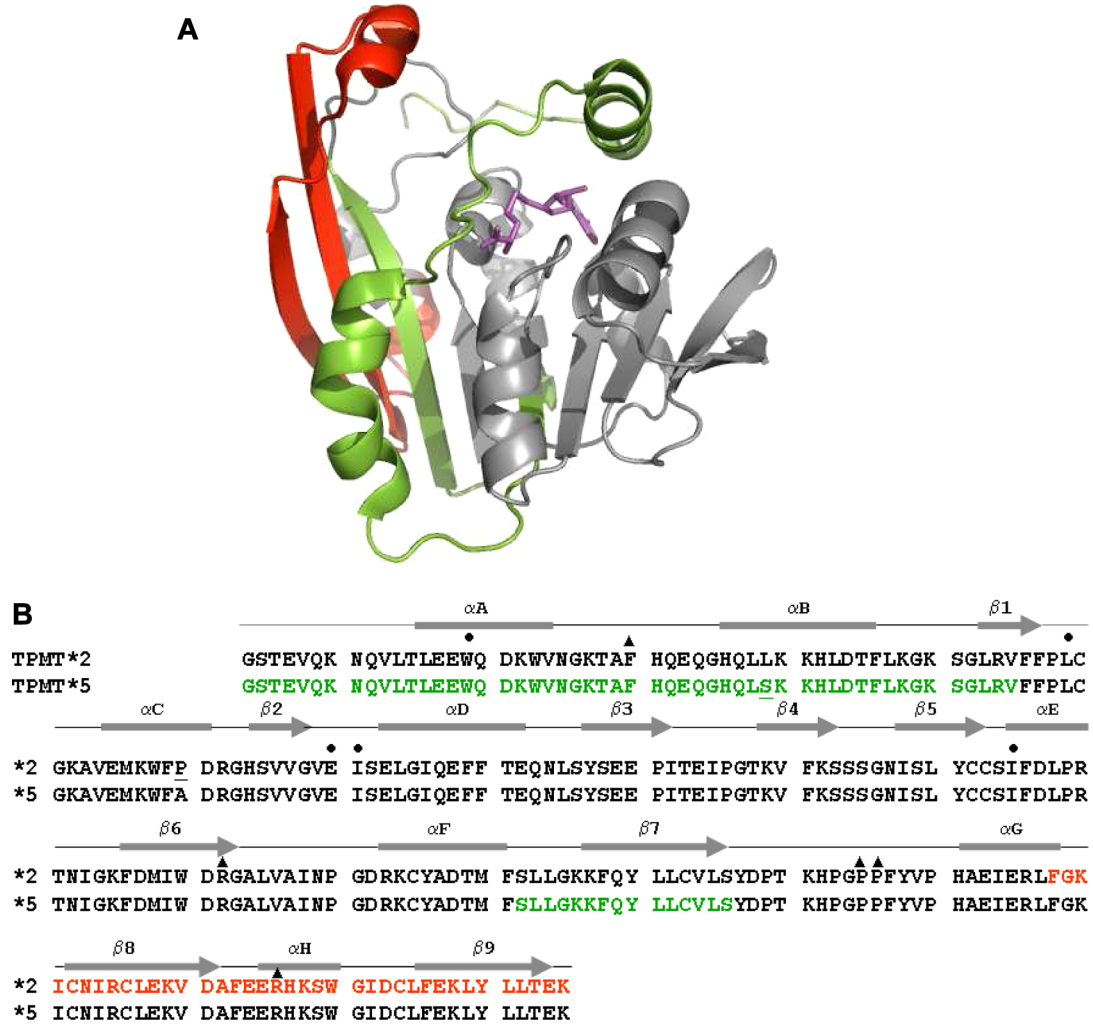

Figure 8. (A) Three-dimensional representation of stable regions in TPMT*2 (red) and TPMT*5 (green). Regions were defined as stable if they showed less than 5% relative propensity to cleave within 10 min and included more than two potential cleavage sites. (B) Amino acid sequences illustrating the stable regions of TPMT*2 (red) and TPMT*5 (green) and the corresponding secondary structure elements. Residues involved in binding cofactor SAH (●) and the substrate 6-MP (▲) are indicated. The figure is based on structural information about human[6] and murine[29] TPMT obtained using PDB entries 2BZG and 3BGD.

only local changes that are manifested by the loss of ANS binding and not by the stability of the secondary structure.

The balance among folding, misfolding, and aggregation of TPMT variants has been discussed previously,[27] and it has been suggested that many variants, including TPMTwt, have a tendency to aggregate.[9,27] Thus it seems that the substitution per se does not impair the enzymatic activity of TPMT but rather strengthens the tendency to aggregate, thereby lowering the availability of active molecules in vivo. Protein aggregation is well studied in the field of Alzheimer's disease[28] and has been proposed to be a route to degradation of TPMT.[27] Traditionally, the two well-established fluorophores, Congo red[29] and thioflavin T,[30] have been used to detect protein aggregates, although a repertoire of other fluorescent molecules is available today, including the LCOs.[25] After our right-angle light scattering experiment had indicated the formation of TPMTwt, TPMT*2, and TPMT*5 aggregates, LCO h-FTAA was used to achieve more qualitative measurements. The results showed that the protein aggregates differed with regard to both their morphology and their affinity for h-FTAA (Figure 6). TPMT*2 and TPMT*5 were the variants that formed fibrils; this was seen in the h-FTAA spectrum as distinct peaks at wavelengths characteristic of fibril binding.[25] However, TPMT*2 had a higher fluorescence intensity, indicating stronger binding of h-FTAA. The strong tendency to aggregate was also indicated by the low stability monitored with both the secondary and tertiary structure probes. By applying a limited proteolysis approach, we were able to pinpoint regions in the structure that might be responsible for the stability changes and reduced enzyme activity in TPMT*2 and TPMT*5.

From the crystal structures of murine TPMT[31] and on the basis of the high degree of sequence homology to the human TPMT, residues involved in the binding of cofactor SAH (W33, L69, E90, I91, and I135) as well as the substrate 6-MP (F40, R152, P195, P196, and R226) are illustrated for human TPMT (Figure 8B). Notably, three of these residues (W33, F40, and L69) are potential cleavage sites for chymotrypsin and preferentially cleaved in TPMT*2 (Figure 7). This agrees with recent in silico modeling experiments with TPMT*2 that suggested that the final turn of helix αC was disrupted to allow the A80P mutation, which thereby altered the secondary structure, and those assessments also revealed an increase in the solvent-accessible surface area of the SAM-binding site.[8] The cleavage pattern of TPMT*2 displayed a stable C-terminus at

dx.doi.org/10.1021/bi300377d | *Biochemistry* 2012, 51, 5912−5920

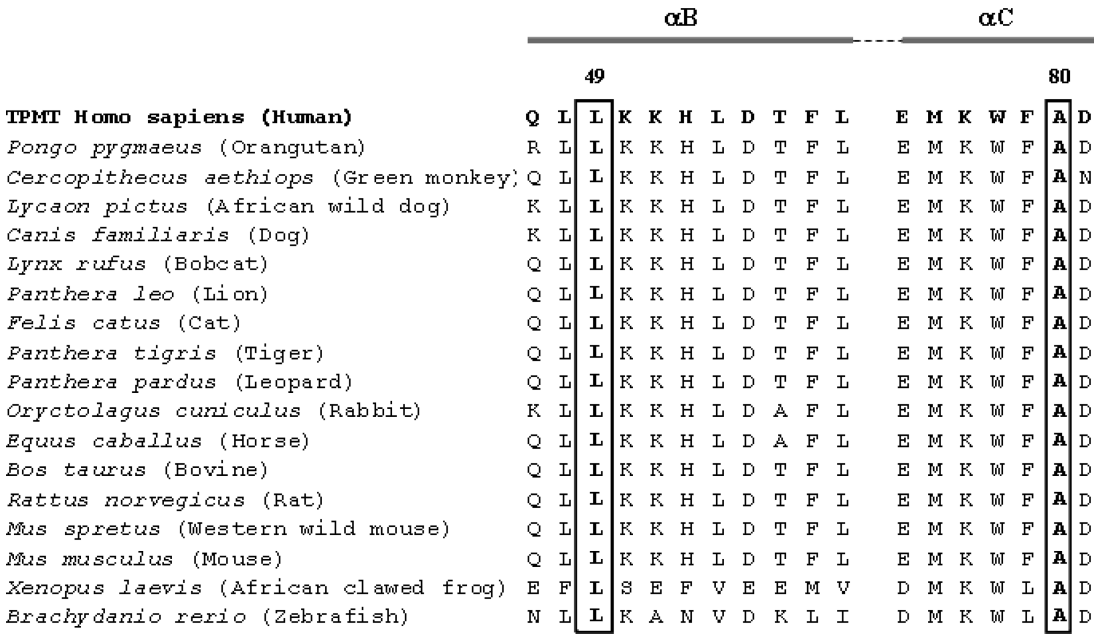

Figure 9. Alignment of TPMT sequences used in SIFT score analysis.[24] The illustrated boundaries of the sequences represent the helix region for positions 49 and 80, respectively, according to the human TPMT structure.[6]

residues 208−245 that was inaccessible for chymotrypsin cleavage. One reasonable explanation might be protein oligomerization, causing residue protection in the C-terminus, as indicated by the far-UV CD spectrum.

Limited proteolysis experiments in this study revealed a stable N-terminal region, at residues 15−65 of TPMT*5, displaying rigidity in the tertiary structure. Of particular interest in our study, three of the residues in TPMT*5 that are inaccessible to cleavage, Phe40, Leu48 (in TPMTwt the neighboring Leu49 in the mutational position is also cleaved), and Phe56, are situated in or near the active site loop. Hence, the low enzyme activity of TPMT*5 can be explained by local structural changes in the active site region and not by decreased stability.

The crystal structure of mouse TPMT[31] has revealed changes in flexibility of the active site loop between residues Arg31 and Gln55 (corresponding to residues Ala39−His52 in the human protein). This loop comprises helix αB harboring the L49S mutation (TPMT*5), which supports our finding that its flexibility might be disrupted by the mutation.

In conclusion, new variants of TPMT have traditionally been discovered in patients with low TPMT enzyme activity. Also, determination of the structure of human TPMT[6] has revealed that the positions of the allelic variants are distributed throughout the entire protein.

Our study has clearly shown that TPMT*2 and TPMT*5 have different structural characteristics that give rise to the low enzyme activity that these variants exhibit in vivo. TPMT*2 is less stable and more flexible and is more prone to aggregate. TPMT*5, on the other hand, is more stable, and its low enzyme activity is instead the result of local structural changes in the active site region. The results presented here show the importance of a repertoire of biophysical techniques for exploring and understanding the structural differences between TPMT variants on a molecular level and for complementing in vivo studies.

AUTHOR INFORMATION

Corresponding Author

*Phone: +46 (0) 13 28 57 05. E-mail: lgmar@ifm.liu.se.

Present Addresses

[‖]Institute of Neuropathology, Zurich University Hospital, CH-8091 Zürich, Switzerland.

[⊥]Institute of Structural Biology, Helmholtz Zentrum München, D-857 64 Neuherberg, Germany, and Munich Center for Integrated Protein Science at the Chair of Biomolecular NMR, Department Chemie, Technische Universität München, D-857 47 Garching, Germany.

Funding

This work was supported by grants from the Swedish Childhood Cancer Foundation. J.H. gratefully acknowledges a postdoctoral fellowship from the Swedish Research Council and a long-term fellowship from EMBO. P.W. and T.K. are enrolled in the doctoral program Forum Scientium.

Notes

The authors declare no competing financial interest.

ABBREVIATIONS

ANS, anilinonaphthalene sulfonate; ALL, acute lymphoblastic leukemia; CD, circular dichroism; h-FTAA, heptaformic thiophene acetic acid; IBD, inflammatory bowel disease; LCOs, luminescent conjugated oligothiophenes; PDB, Protein Data Bank; SAM, *S*-adenosylmethionine; SAH, *S*-adenosylhomocysteine; TCEP, tris(2-carboxyethyl)phosphine; T_m, thermal transition midpoint of denaturation; TPMT, thiopurine *S*-methyltransferase; TPMTwt, wild-type TPMT.

REFERENCES

(1) Dervieux, T., Blanco, J. G., Krynetski, E. Y., Vanin, E. F., Roussel, M. F., and Relling, M. V. (2001) Differing contribution of thiopurine methyltransferase to mercaptopurine versus thioguanine effects in human leukemic cells. *Cancer Res. 61*, 5810−5816.

(2) Coulthard, S. A., Hogarth, L. A., Little, M., Matheson, E. C., Redfern, C. P., Minto, L., and Hall, A. G. (2002) The effect of

thiopurine methyltransferase expression on sensitivity to thiopurine drugs. *Mol. Pharmacol. 62*, 102−109.
(3) Garat, A., Cauffiez, C., Renault, N., Lo-Guidice, J. M., Allorge, D., Chevalier, D., Houdret, N., Chavatte, P., Loriot, M. A., Gala, J. L., and Broly, F. (2008) Characterisation of novel defective thiopurine S-methyltransferase allelic variants. *Biochem. Pharmacol. 76*, 404−415.
(4) Evans, W. E., Horner, M., Chu, Y. Q., Kalwinsky, D., and Roberts, W. M. (1991) Altered mercaptopurine metabolism, toxic effects, and dosage requirement in a thiopurine methyltransferase-deficient child with acute lymphocytic leukemia. *J. Pediatr. 119*, 985−989.
(5) Kaskas, B. A., Louis, E., Hindorf, U., Schaeffeler, E., Deflandre, J., Graepler, F., Schmiegelow, K., Gregor, M., Zanger, U. M., Eichelbaum, M., and Schwab, M. (2003) Safe treatment of thiopurine S-methyltransferase deficient Crohn's disease patients with azathioprine. *Gut 52*, 140−142.
(6) Wu, H., Horton, J. R., Battaile, K., Allali-Hassani, A., Martin, F., Zeng, H., Loppnau, P., Vedadi, M., Bochkarev, A., Plotnikov, A. N., and Cheng, X. (2007) Structural basis of allele variation of human thiopurine-S-methyltransferase. *Proteins 67*, 198−208.
(7) Schubert, H. L., Blumenthal, R. M., and Cheng, X. (2003) Many paths to methyltransfer: A chronicle of convergence. *Trends Biochem. Sci. 28*, 329−335.
(8) Rutherford, K., and Daggett, V. (2008) Four human thiopurine S-methyltransferase alleles severely affect protein structure and dynamics. *J. Mol. Biol. 379*, 803−814.
(9) Wang, L., Nguyen, T. V., McLaughlin, R. W., Sikkink, L. A., Ramirez-Alvarado, M., and Weinshilboum, R. M. (2005) Human thiopurine S-methyltransferase pharmacogenetics: Variant allozyme misfolding and aggresome formation. *Proc. Natl. Acad. Sci. U.S.A. 102*, 9394−9399.
(10) Salavaggione, O. E., Wang, L., Wiepert, M., Yee, V. C., and Weinshilboum, R. M. (2005) Thiopurine S-methyltransferase pharmacogenetics: Variant allele functional and comparative genomics. *Pharmacogenet. Genomics 15*, 801−815.
(11) Krynetski, E. Y., Schuetz, J. D., Galpin, A. J., Pui, C. H., Relling, M. V., and Evans, W. E. (1995) A single point mutation leading to loss of catalytic activity in human thiopurine S-methyltransferase. *Proc. Natl. Acad. Sci. U.S.A. 92*, 949−953.
(12) Tai, H. L., Krynetski, E. Y., Schuetz, E. G., Yanishevski, Y., and Evans, W. E. (1997) Enhanced proteolysis of thiopurine S-methyltransferase (TPMT) encoded by mutant alleles in humans (TPMT*3A, TPMT*2): Mechanisms for the genetic polymorphism of TPMT activity. *Proc. Natl. Acad. Sci. U.S.A. 94*, 6444−6449.
(13) Ujiie, S., Sasaki, T., Mizugaki, M., Ishikawa, M., and Hiratsuka, M. (2008) Functional characterization of 23 allelic variants of thiopurine S-methyltransferase gene (TPMT*2−*24). *Pharmacogenet. Genomics 18*, 887−893.
(14) Spire-Vayron de la Moureyre, C., Debuysere, H., Sabbagh, N., Marez, D., Vinner, E., Chevalier, E. D., Lo Guidice, J. M., and Broly, F. (1998) Detection of known and new mutations in the thiopurine S-methyltransferase gene by single-strand conformation polymorphism analysis. *Hum. Mutat. 12*, 177−185.
(15) Appell, M. L., Wennerstrand, P., Peterson, C., Hertervig, E., and Mårtensson, L. G. (2010) Characterization of a novel sequence variant, TPMT*28, in the human thiopurine methyltransferase gene. *Pharmacogenet. Genomics 20*, 700−707.
(16) Hennig, J., Ottosson, L., Andresen, C., Horvath, L., Kuchroo, V. K., Broo, K., Wahren-Herlenius, M., and Sunnerhagen, M. (2005) Structural organization and Zn^{2+}-dependent subdomain interactions involving autoantigenic epitopes in the Ring-B-box-coiled-coil (RBCC) region of Ro52. *J. Biol. Chem. 280*, 33250−33261.
(17) Hennig, J., Bresell, A., Sandberg, M., Hennig, K. D., Wahren-Herlenius, M., Persson, B., and Sunnerhagen, M. (2008) The fellowship of the RING: The RING-B-box linker region interacts with the RING in TRIM21/Ro52, contains a native autoantigenic epitope in Sjogren syndrome, and is an integral and conserved region in TRIM proteins. *J. Mol. Biol. 377*, 431−449.
(18) Hennig, J., Hennig, K. D., and Sunnerhagen, M. (2008) MTMDAT: Automated analysis and visualization of mass spectrometry data for tertiary and quaternary structure probing of proteins. *Bioinformatics 24*, 1310−1312.
(19) Ng, P. C., and Henikoff, S. (2003) SIFT: Predicting amino acid changes that affect protein function. *Nucleic Acids Res. 31*, 3812−3814.
(20) Freskgård, P. O., Mårtensson, L. G., Jonasson, P., Jonsson, B. H., and Carlsson, U. (1994) Assignment of the contribution of the tryptophan residues to the circular dichroism spectrum of human carbonic anhydrase II. *Biochemistry 33*, 14281−14288.
(21) Mårtensson, L. G., Jonsson, B. H., Freskgård, P. O., Kihlgren, A., Svensson, M., and Carlsson, U. (1993) Characterization of folding intermediates of human carbonic anhydrase II: Probing substructure by chemical labeling of SH groups introduced by site-directed mutagenesis. *Biochemistry 32*, 224−231.
(22) Mårtensson, L. G., Karlsson, M., and Carlsson, U. (2002) Dramatic stabilization of the native state of human carbonic anhydrase II by an engineered disulfide bond. *Biochemistry 41*, 15867−15875.
(23) Willcock, D. F., Dryden, D. T., and Murray, N. E. (1994) A mutational analysis of the two motifs common to adenine methyltransferases. *EMBO J. 13*, 3902−3908.
(24) Powell, L. M., Dryden, D. T., Willcock, D. F., Pain, R. H., and Murray, N. E. (1993) DNA recognition by the EcoK methyltransferase. The influence of DNA methylation and the cofactor S-adenosyl-L-methionine. *J. Mol. Biol. 234*, 60−71.
(25) Klingstedt, T., Åslund, A., Simon, R. A., Johansson, L. B., Mason, J. J., Nyström, S., Hammarstrom, P., and Nilsson, K. P. (2011) Synthesis of a library of oligothiophenes and their utilization as fluorescent ligands for spectral assignment of protein aggregates. *Org. Biomol. Chem. 9*, 8356−8370.
(26) Klingstedt, T., and Nilsson, K. P. (2011) Conjugated polymers for enhanced bioimaging. *Biochim. Biophys. Acta 1810*, 286−296.
(27) Feng, Q., Vannaprasaht, S., Peng, Y., Angsuthum, S., Avihingsanon, Y., Yee, V. C., Tassaneeyakul, W., and Weinshilboum, R. M. (2010) Thiopurine S-methyltransferase pharmacogenetics: Functional characterization of a novel rapidly degraded variant allozyme. *Biochem. Pharmacol. 79*, 1053−1061.
(28) Selkoe, D. J. (2001) Alzheimer's disease: Genes, proteins, and therapy. *Physiol. Rev. 81*, 741−766.
(29) Ladewig, P. (1945) Double refringence of the Amyloid-Congo-Red-Complex in histologi sections. *Nature 156*, 81−82.
(30) Vassar, P. S., and Culling, C. F. (1959) Fluorescent stains, with special reference to amyloid and connective tissues. *Arch. Pathol. 68*, 487−498.
(31) Peng, Y., Feng, Q., Wilk, D., Adjei, A. A., Salavaggione, O. E., Weinshilboum, R. M., and Yee, V. C. (2008) Structural basis of substrate recognition in thiopurine S-methyltransferase. *Biochemistry 47*, 6216−6225.
(32) *The PyMOL molecular graphics system*, version open-source PyMOL 1.1.x (2010) Schrödinger LLC, New York.